2025 IEEE/ASME International Conference on Advanced Intelligent Mechatronics (AIM) | 979-8-3315-3342-7/25/$31.00 ©2025 IEEE | DOI: 10.1109/AIM64088.2025.11175716

Hybrid Physics-data Driven Unified Modeling of Switching ElectroMechanical Brake Systems

Huaicheng Yao, Teng Zuo, Wenpeng Wei*, Guodong Yin*

***Abstract*—Modeling of ElectroMechanical Brake (EMB) system is fundamental for the safety control of intelligent or autonomous vehicles. However, traditional physics-based EMB system modeling can be challenging due to requirement of precise parameters value and the switching among multi-stage working process of the EMB system. This paper proposes a hybrid physics-data driven modeling approach based on the Linear-Parameter-Varying (LPV) state space representation to describe the multi-stage working process of the EMB system in a unified model framework. The unified model starts with a traditional physical-based EMB system model, where multiple system parameters are presented, while the friction torque and the hysteresis braking force is modeled by switching functions; Then, the physical model is transformed into a quasi-LPV state space with motor speed appeared in the scheduling parameter vector; The system matrices are then identified through data, avoiding the precise value of each individual system parameters. The effectiveness of the unified model is then validated using experiment data, showing the smoothness and accuracy of the proposed model.**

***Index Terms*—ElectroMechanical Brake; Brake-by-wire; Autonomous Vehicles; Hybrid Physics-Data Modeling; Switching Systems**

I. Introduction

Electromechanical braking (EMB) systems have received unprecedented attention in autonomous vehicles [1], attributes to its potential of significantly enhancing the safety, stability and energy utilization efficiency [2]. They offer expeditious force response and prominent force control precision across various operation ranges, particularly under critical driving conditions [3]. On top of them, modeling of EMB systems lays as a solid foundation. Although the physical structure of EMB system is simple, accurately modeling the EMB system stands as a complex and non-trivial task [4]. The primary challenges are embodied in two key aspects: the stage switching behavior of the system and the time-varying nature of its parameters. As a result, it is of significant importance to develop high precision EMB system models to guarantee its potentials.

The first challenge in precise modeling of the EMB system lies in the necessity of multiple stages to characterize the working principle [5]. Generally, a complete braking process consists of five stages [6], i.e., gap elimination, force clamping, force holding, force releasing, and gap regeneration, as shown in Figure 1. Each stage is described concisely below:

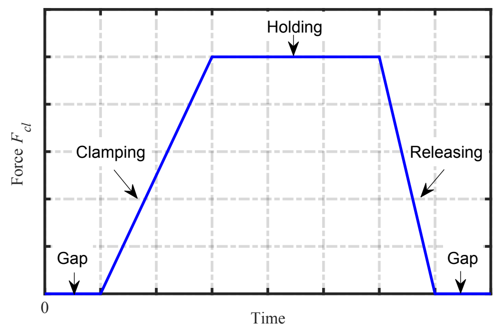

Fig. 1 Multiple Working Stages of EMB System.

(1) Gap elimination stage: An appropriate brake gap is necessary in normal driving condition. Upon receiving a braking command, the braking system needs to eliminate this gap before generating any braking force;

(2) Force Clamping stage: as the brake pad deforms under increasing thrust from the brake motor, the clamping force elevates according to the brake command;

(3) Force Holding stage: once the actual brake force reaches the desired braking force, the motor enters a stall condition to ensure consistent and sustained braking performance;

(4) Force Releasing stage: when the braking process ends, the braking motor reverses its rotational direction to decreases the clamping force;

(5) Gap regeneration stage: when the braking process is terminated, the motor further retracts to remove brake force and reformulates the gap, preparing for future braking events.

It is noted that there is a switch between no load and braking force load condition when the EMB system switches between the gap phase (gap elimination and gap regeneration) and the braking phase (clamping and releasing). Also, during the clamping and releasing stages, the direction of friction force is noted to change due to the direction change of angular velocity [7]. Furthermore, the braking force, exhibiting obvious switching property [8], cannot be adequately described by a single characteristic curve due to hysteresis effect. To make things worse, in the force holding stage, the friction displays quasi-static stick-slip behavior [9], where the friction torque may change direction regardless of the stationary status of EMB. To sum up, the EMB system is fundamentally recognized as a multi-stage switching system that poses great challenges for system dynamic modeling.

This work is supported partially by the National Natural Science Foundation of China under Grant 52402467 and Grant 52394263, by the Natural Science Foundation of Jiangsu Province under Grants NO. BK20241324, by the "Shanghai Magnolia Talent Plan Pujiang Project 24PJB019" and by the "Southeast University Interdisciplinary Research Program for Young Scholars".

The authors are with School of Mechanical Engineering, Southeast University, Nanjing, Jiangsu, China (e-mail: {yaohuaicheng; zuoteng; weiwenpeng; ygd}@seu.edu.cn).

*Corresponding author.

The second challenge in the EMB system modeling lies in the availability and reliability of its system parameters. Although each working stage is clearly defined, the establishment of the system model based on traditional physics principles depends on the accuracy of system parameters [10], such as motor resistance, inductance, flux linkage, equivalent rotational inertia, and motor constants and so on. However, on one hand, EMB system parameters identification may require extensive experimental work [11] [12]. And the possibly time-varying characteristics of these parameters introduced by environmental factors such as temperature changes complicate the calibration process, making it more difficult to ensure their accuracy [13]; On the other hand, considerable effort is required to appropriately set switching thresholds to accommodate for the multiphase operation of EMB systems, especially when the switching signals are poisoned by measurement noises. Furthermore, during the force holding stage, the clamping force is significantly affected by static friction [8]. Consequently, quantitatively modeling the complex dynamic behavior of EMB system under unreliable parameters is challenging.

In summary, the EMB system is a condition-based switching system wherein the model switch may be triggered many times near switching points within a short period, significantly reducing the model fidelity. At the same time, the accuracy of traditional physics-based models severely rely on the reliability of system parameter calibration. Yet, existing physical modeling efforts mainly concentrate on braking process and failed to account for parameters variation.

To address these issues, this paper proposes a unified modeling framework for the entire operational stage of the EMB system. This integrated framework employs a hybrid physics-data-driven approach that combines both the physical laws of EMB system and the operational data across multiple conditions. The contributions of the paper are as follows:

(1) Develop a hybrid physics-data driven unified model for EMB systems by integrating the motor physics and the operational data through the linear parameter-varying (LPV) modeling theory. This approach eliminates the requirement for parameters calibration, yet preserves the physics in the model;

(2) Propose a unified modeling framework covering entire operational stage for the first time for the EMB system without dedicate switching logic. The model switching is captured by the selection of the scheduling parameter, i.e. the sign function of the motor speed that encodes the switching of friction torque and braking force.

The rest of the paper is organized as follows. Section II reviews the physics-based system modeling of the EMB system; In Section III, the hybrid physics-data driven unified modeling approach using Linear Parameter Varying representation is presented; Experimental results are presented in Sections IV. Some conclusions are given in Section V.

II. Traditional Physical Model of EMB System

In this section, the working principle and the physics-based system modeling of the EMB system is reviewed.

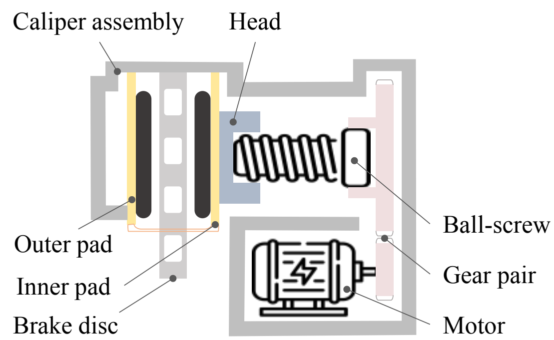

Fig. 2 Schematic diagram of EMB.

A. Working Principle of EMB System

Fig. 2 illustrates the structural diagram of the EMB system. The EMB system consists of the driving unit (electric motor), the torque amplification mechanism (gear reduction unit), the motion conversion component (the ball screw), and the brake components (the brake pads and brake disc assembly). The complete working cycle of the EMB system is a multi-stage process that includes brake gap elimination, braking force application, braking force holding, braking force release, and brake gap regeneration.

In each phase of the working cycle, the system's operating state and control strategy differs, requiring different models to reflect system dynamic behavior. As a result, the system model needs to switch across distinct operational conditions.

B. Traditional Physics-based Modeling of the EMB System

The system dynamics of EMB systems typically consist of both the electrical and mechanical loops [14], which can be described in a simple way as below.

$$\begin{aligned} L\frac{di_q}{dt} &= v - Ri_q - k_w w_m \\ J_m \dot{w}_m &= k_m i_q - T_f - T_L \end{aligned} \tag{1}$$

where i_q is the motor current; L is the motor inductance; R is the motor resistance; w_m is the motor angular speed; k_w is the Back EMF Constant; v is the motor current; J_m is the motor inertia; k_m is the torque constant; T_f is the friction torque; and T_L is the load torque related to the braking force.

It is mentioned in [10] that the friction torque depends on the clamping force and is usually modelled as a switching function decided by motion status, as follows.

$$T_f = \begin{cases} (\gamma F_{cl} + T_{f0}) sign(w_m) + b_f w_m & w_m \neq 0 \\ k_m i_q - T_L & w_m = 0 \& T_e < T_s \\ T_s \mathrm{sign}(w_m) & w_m = 0 \& T_e \geq T_s \end{cases} \tag{2}$$

where γ is the clamping force dependent coefficient; T_{f0} is the torque offset; b_f is the viscous friction coefficient; and T_s is the stick friction torque. Reference [10] also noted that γ may be time-varying.

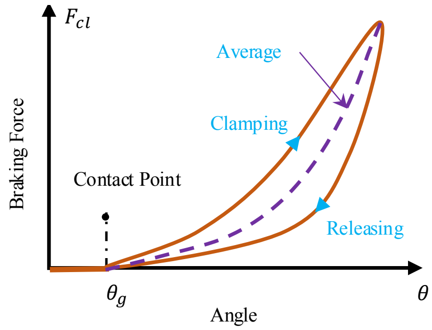

Fig. 3 Relationship between braking force and motor angle

The load torque is related to the clamping force directly through the entire motion conversion chain, and the typical relationship can be expressed as:

$$T_L = k_{cl} F_{cl}, \quad k_{cl} = \frac{P_h}{2\pi i_g \eta_g} \tag{3}$$

where k_{cl} is the clamping force gain that is related to ball-screw pitch P_h, reduction gear ratio i_g and transmission efficiency η_g; F_{cl} denotes the clamping force.

The most widely used clamping force estimation method is to fit the relationship between the clamping force and the motor angle using a polynomial function [15]. Considering the hysteresis effect between braking and releasing, see Fig. 3, the general form of the polynomial can be expressed as follows.

$$F_{cl} = \begin{cases} 0 & \theta_m < \theta_g \\ p_{0,c} + \sum_{i=1}^{n_p} p_{i,c}\theta_m^i & \theta_m \geq \theta_g \,\&\, w_m \geq 0 \\ p_{0,r} + \sum_{i=1}^{n_p} p_{i,r}\theta_m^i & \theta_m \geq \theta_g \,\&\, w_m < 0 \end{cases} \tag{4}$$

where $p_{i,c/r}(i = 0, 1, \ldots, n_p)$ are polynomial coefficients needs to be identified with pre-collected experimental data, and n is the order of the polynomial function.

In summary, accurately modeling of the EMB system based on physical principles relies on the parameters involved from equations (1) to (4). These parameters can be categorized into system parameters, friction-related parameters, and load-dependent parameters, as shown in Table I.

TABLE I: EMB modeling parameters

parameter categories	parameters
system parameters	$L, R, k_w, J_m, k_m, P_h, i_g, \eta_g$
friction parameters	γ, T_{f0}, b_f, T_s
external parameters	F_{cl}

Remark 1: The above equations cover the entire working cycle of the EMB system as shown in Fig. 1, where the force equals to 0 in (4) covers the gap phases, and the other branches in (2) and (4) covers braking (clamping, holding and releasing) phases. The model is essentially a switching system, and each phase is represented by a different model according to the conditions change.

Remark 2: Parameters in Table I typically require a large amount of experimental data and effort for offline calibration, a process that is both time-consuming and labor-intensive, and nontheless, the results may lack adaptability.

Remark 3: The switching behavior in friction torque and clamping force is determined by the sign of motor speed. Due to the existence of measurement noise, it is impossible that the speed can be measured as exact zero and there may exist oscillation when the speed is close to 0. Although a threshold other than 0 can be utilized, discontinuity at the instnace of switching is unavoidable.

III. Hybrid Physics-Data Driven Unified Modeling

In this section, a unified model framework is established based on the fusion of physics-based and data-driven modeling methods, avoiding the parameters calibration and switching discontinuity issues in traditional physics-based modeling.

A. Unified Physical Model of the EMB System

The force characteristic curve order is selected to be $n_p = 2$, and a unified representation of the force characteristic is proposed taking the braking and releasing process into account.

$$\begin{aligned} F_{cl} &= p_0 + p_1\theta_m + p_2\theta_m^2 \\ p_i &= p_{i,p} + p_{i,m}\mathrm{sign}(w_m), \quad i = 0, 1, 2 \\ p_{i,p} &= \frac{p_{i,b} + p_{i,r}}{2}, \quad p_{i,m} = \frac{p_{i,b} - p_{i,r}}{2} \end{aligned} \tag{5}$$

where $p_{i,b}$ and $p_{i,r}$ are defined in (4). By using (5), the clamping force with hysteresis can be described by a single expression, instead of the switching function (4).

Combining (1) to (5), the dynamic equations of the EMB system can be derived below.

$$\begin{aligned} L\frac{di_q}{dt} &= -Ri_q - k_w w_m + v \\ \dot{\theta}_m &= w_m \\ J_m\dot{w}_m &= k_m i_q - k_{f0} v\,\mathrm{sign}(w_m) - b_f w_m - (k_{cl} + \gamma\,\mathrm{sign}(w_m))F_{cl} \\ \dot{F}_{cl} &= (p_{1,p} + p_{1,m}\mathrm{sign}(w_m))w_m + 2(p_{2,p} + p_{2,m}\mathrm{sign}(w_m))w_m\theta_m \end{aligned} \tag{6}$$

where θ_m is motor angle; and k_{f0} is a coefficient (possibly time varying) that satisfies $T_{f0} = k_{f0}v$ if v is not zero. Note that v equals zero means the system is not working, then no modeling is needed. As a result, the above relation holds true and the data driven approach in the next subsection will be introduced to deal with the unknown parameters.

B. Unified Hybrid Model of the EMB System

To deal with time-varying parameters and the switching effects in the EMB systems, the hybrid physics-data modeling of the EMB system based on Linear-Parameter-Varying (LPV) representation is proposed.

Select states as $x = \left[i_q, \theta_m, w_m, F_{cl}\right]^T$, input as $u = v$, system (6) can be transformed into a LPV state space representation with the scheduling parameter vector $\rho = [\text{sign}(w_m), \text{sign}(w_m)w_m]^T$ as follows.

$$\begin{aligned} \dot{x} &= A(\rho)x + B(\rho)u \\ A(\rho) &= A_0 + A_1\rho_1 + A_2\rho_2 \\ B(\rho) &= B_0 + B_1\rho_1 + B_2\rho_2, \end{aligned} \tag{7}$$

Detailed matrices representations are omitted due to paper length limit. In this paper, we assume that the force F_{cl} can be obtained through a force sensor.

To facilitate the data-driven system formulation, the LPV system (7) is discretized as follows.

$$x_{k+1} = A_k(\rho_k)x_k + B_k(\rho_k)u_k \tag{8}$$

where each signal with discrete time step k represents the discrete counterpart of the continuous signals.

Introducing the Kronecker product operation, and remember that $B_{2k} = 0$, the system is further transformed to below format.

$$\begin{aligned} x_{k+1} =& \mathcal{A}_k \begin{bmatrix} x_k \\ \rho_k \otimes x_k \end{bmatrix} + \mathcal{B}_k \begin{bmatrix} u_k \\ \rho_{1k} \otimes u_k \end{bmatrix} \\ \mathcal{A}_k =& \begin{bmatrix} A_{0k} & A_{1k} & A_{2k} \end{bmatrix} \\ \mathcal{B}_k =& \begin{bmatrix} B_{0k} & B_{1k} \end{bmatrix} \end{aligned} \tag{9}$$

In view of (9), it is obvious that if the matrix $\begin{bmatrix} \mathcal{A}_k & B_k \end{bmatrix}$ can be identified, the dynamic model of the EMB can be obtained. Therefore, in order to achieve this goal, the data trace of system state vector x_k, system u_k and scheduling parameter vector ρ_k with data length N are assumed to be collected, which is denoted as data set $\mathcal{D}_{EMB} = \{x_k, u_k, \rho_k\}$. Define the data matrices with below notations.

$$\begin{aligned} \mathbf{U} &= \begin{bmatrix} u_1^d & u_2^d & \dots & u_{N-1}^d \end{bmatrix} \in \mathcal{R}^{n_u \times (N-1)} \\ \mathbf{X} &= \begin{bmatrix} x_1^d & x_2^d & \dots & x_{N-1}^d \end{bmatrix} \in \mathcal{R}^{n_x \times (N-1)} \\ \mathbf{X}^+ &= \begin{bmatrix} x_2^d & x_3^d & \dots & x_N^d \end{bmatrix} \in \mathcal{R}^{n_x \times (N-1)} \\ \mathbf{X}(\rho_k) &= \begin{bmatrix} \rho_1^d \otimes x_1^d & \dots & \rho_{N-1}^d \otimes x_{N-1}^d \end{bmatrix} \in \mathcal{R}^{n_\rho n_x \times (N-1)} \\ \mathbf{U}(\rho_k) &= \begin{bmatrix} \rho_{1,1}^d \otimes u_1^d & \dots & \rho_{1,N-1}^d \otimes u_{N-1}^d \end{bmatrix} \in \mathcal{R}^{n_u \times (N-1)} \end{aligned} \tag{10}$$

where N is the number of data points collected, the superscript d denotes discrete-time samples.

As a result, the above data matrices obey dynamics (9), resulting (11) holds true.

$$\mathbf{X}^+ = \underbrace{\begin{bmatrix} \mathcal{A}_k & B_k \end{bmatrix}}_{\Gamma} \begin{bmatrix} \mathbf{X}' & \mathbf{X}'(\rho_k) & \mathbf{U}' & \mathbf{U}'(\rho_k) \end{bmatrix}^T \tag{11}$$

Apparently, with above relationship, the system matrices can be obtained easily through least-square regression as below.

$$\Gamma = \mathbf{X}^+ \begin{bmatrix} \mathbf{X} \\ \mathbf{X}(\rho_k) \\ \mathbf{U} \\ \mathbf{U}(\rho_k) \end{bmatrix}^T \left(\begin{bmatrix} \mathbf{X} \\ \mathbf{X}(\rho_k) \\ \mathbf{U} \\ \mathbf{U}(\rho_k) \end{bmatrix} \begin{bmatrix} \mathbf{X} \\ \mathbf{X}(\rho_k) \\ \mathbf{U} \\ \mathbf{U}(\rho_k) \end{bmatrix}^T \right)^{-1} \tag{12}$$

This completes the hybrid-physic-data driven EMB system modeling.

Remark 4: The above modeling technique is accomplished by the collected data trace from EMB system with various operation conditions, and EMB system parameters listed in Table I are not required. The requirements on input data are detailed in [16].

Remark 5: By selecting the scheduling parameter vector with respect to $\text{sign}(w_m)$ in the hybrid physics-data framework, the switching nature of the EMB system appeared in friction torque (2) and clamping force (4) are captured through a unified model structure.

IV. Experimental Validation

In this section, the hybrid physics-data model is validated using normalized real vehicle testing data, and the proposed approach is compared with traditional physics-based model. The following points are demonstrated through the comparison.

(1) The accuracy of physical-based EMB system model heavily depends on the accuracy of system parameters and lacks adaptability;

(2) There exists jumping discontinuities at the point of switching for the physical-based model;

(3) The proposed modeling approach models the system dynamics accurately, smoothly and adaptively.

Note that the true values for each signal are normalized.

A. Hybrid LPV Model Learning

The system matrices $\mathcal{A}_k$ and B_k are constructed through the LPV modeling method. In the training process, a measured dataset consisting of current, angular, angular velocity, braking force, and voltage is used, with the data length N in (10) being selected as 8000. The system matrices $\mathcal{A}_k$ and B_k are identified as

$$\begin{aligned} \mathcal{A}_k &= \left[\begin{matrix} 0.96 & 0 & 0 & 0 & 0.01 & 0 \\ 0 & 0.99 & 0 & 0 & 0 & 0 \\ 0.03 & 0 & 0.89 & 0 & -0.02 & 0 \\ -0.55 & -0.17 & 1.30 & 1.00 & -0.06 & 0.45 \end{matrix} \right. \\ &\qquad \left. \begin{matrix} 0.02 & 0 & 0 & 0 & 0 & 0 \\ 0 & 0 & 0 & 0 & 0 & 0 \\ 0.02 & 0 & 0 & 0 & -0.03 & 0 \\ -0.87 & 0 & 0.62 & 0.08 & 0.20 & 0 \end{matrix} \right] \\ \mathcal{B}_k &= \begin{bmatrix} 1.51 & -0.27 & -0.29 \\ 0 & 0.02 & 0 \\ -1.58 & 1.56 & 1.42 \\ 18.33 & 17.84 & -9.45 \end{bmatrix} \end{aligned} \tag{13}$$

Note that elements in $\mathcal{A}_k$ or B_k less than $1e^{-2}$ are set to 0.

The identified matrices $\mathcal{A}_k$ and B_k are subsequently inserted into equation (9) to form the hybrid physics-data LPV model. The model is then compared with the measured signals and physical model to evaluate its accuracy and adaptiveness under different operational scenarios.

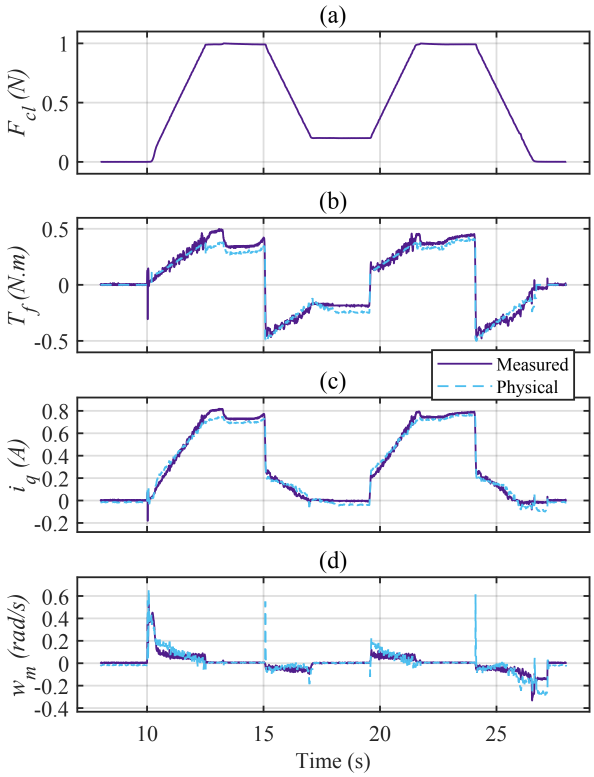

Fig. 4: Physical model with m shape braking: (a) Braking force; (b) Friction torque (c) Input current; (d) Motor speed

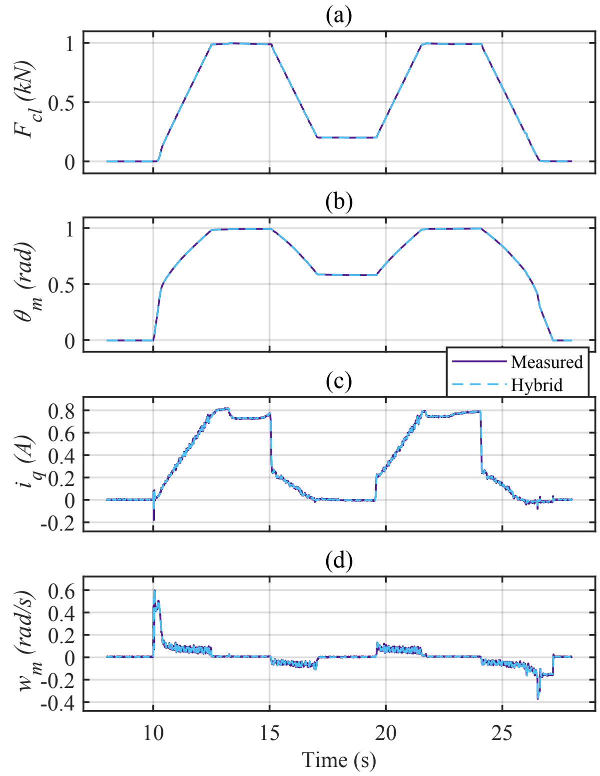

Fig. 5: Hybrid model with m shape braking: (a) Braking force; (b) Motor Angle; (c) Input current; (d) Motor speed

B. Model Validation with "m Shape Force" Scenario

The "m Shape Force" scenario is first employed for validation. Fig. 4 illustrates the performance of the physical model, in which parameters are obtained through offline calibration. The braking force is measured by sensor and the friction torque is presented to demonstrate the effectiveness of parameter calibration. Since the exact signal values are omitted, only RRMSE is used to analyze the estimation errors. Specifically, the RRMSE is 11.34% for motor current and 12.57% for motor angular velocity. It is obvious that when the system switches from force holding to force releasing, there are abrupt jumps in motor speed, see around 15s and 24s in Fig. 4.

Fig. 5 exhibits the hybrid modeling results. It shows the identified hybrid model replicates the state transitions of the EMB system accurately without any abrupt changes. The RRMSE of this method is calculated to be $1.59e^{-5}$%, $2.20e^{-3}$% for motor current and motor angular velocity, respectively, which is much smaller than that of the physical model. This innovative modeling (9) not only achieves exceptional precision, but also smoothly captures the system dynamics (13) without the need for any of the system calibration parameters.

C. Model Validation with "n Shape Force" Scenario

This section displays the validation under the "n shape Force" force scenario. The physical model result is shown in Fig. 6. The system parameters for the model are the same as that in Fig. 4. It can be seen that the physical model in this scenario performances a little bit worse than the "m Shape Force" scenario, especially at instance like 12.8s, 15.4s and 16.6s where jumps are observed. The motor speed also witnesses performance degradation due to multiple switching at instance like 13.8s and 14.8s.

At the same time, the hybrid physics-data model result in Fig. 7 under this scenario performs relatively the same as the previous case. There are also no abrupt jumps presented due to switching. The RRMSEs for current and speed are $7.42e^{-3}$% and $5e^{-3}$%, respectively, whereas the RRMSE values in Fig. 6 are 28.29% and 48.53%. These results again demonstrate the adaptiveness, accuracy and smoothness of the hybrid physics-data model.

V. Conclusion

This paper proposes a hybrid physics-data approach for the smooth, adaptive and accurate unified modeling of a switching nonlinear ElectroMechanical system. The unified model starts with the traditional physical principles of the EMB system, where the switching friction torque and braking force are expressed using single functions; Then, by carefully selecting the states, inputs and scheduling parameters for the system, a Linear-Parameter-Varying representation for the EMB system is reached. This model is a unified representation of the switching physical model; Further, data are integrated into the system dynamics such that the system matrices are identified. The hybrid physics-data EMB system model is obtained without system

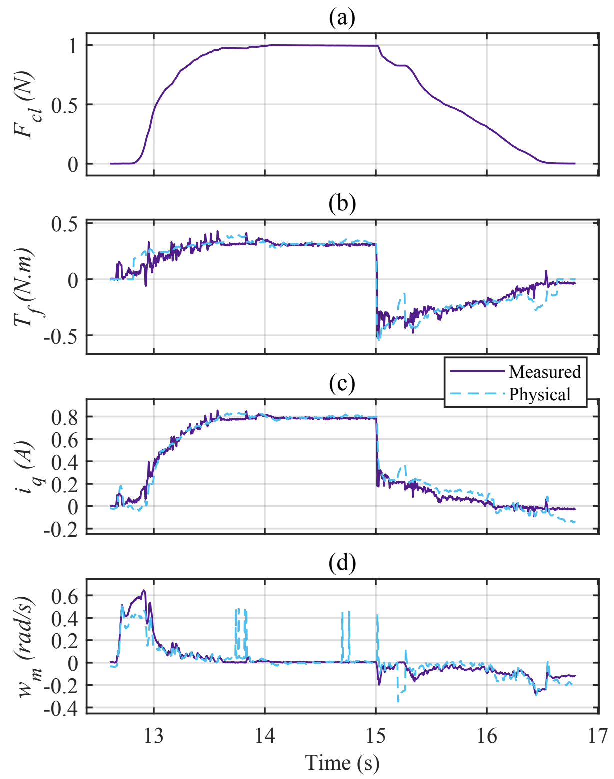

Fig. 6: Physical model with n shape braking: (a) Braking force; (b) Friction torque (c) Input current; (d) Motor speed

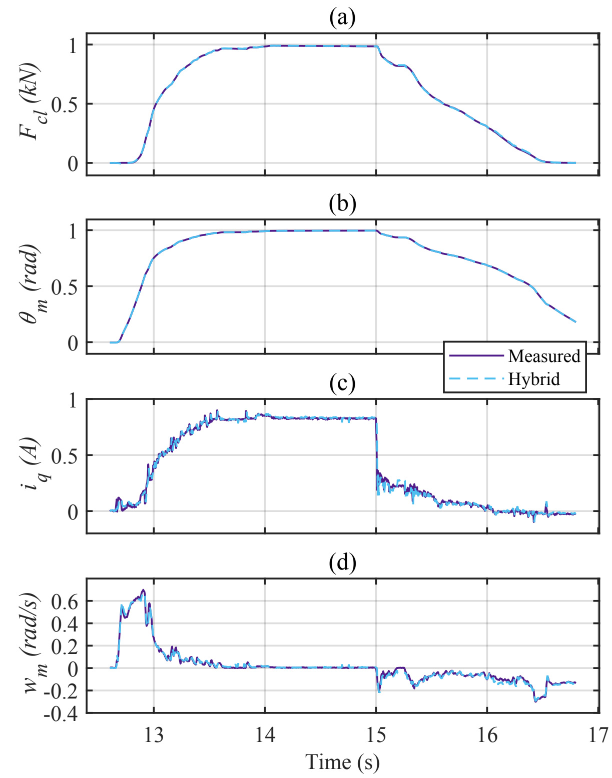

Fig. 7: Hybrid model with n shape braking: (a) Braking force; (b) Motor Angle; (c) Input current; (d) Motor speed

parameters. The performance comparison among the hybrid model, tradition physical model and measurement ground truth confirms that the proposed hybrid model is accurate, smooth and adaptive. The modeling errors are almost negligible. Future work will concentrate on the modeling without using braking force sensors.

References

[1] L. Zhang, Q. Wang, J. Chen, Z.-P. Wang, and S.-H. Li, "Brake-by-wire system for passenger cars: A review of structure, control, key technologies, and application in x-by-wire chassis," *eTransportation*, vol. 18, p. 100292, 2023.

[2] X. Chen, L. Wei, X. Wang, L. Li, Q. Wu, and L. Xiao, "Hierarchical cooperative control of anti-lock braking and energy regeneration for electromechanical brake-by-wire system," *Mechanical Systems and Signal Processing*, vol. 159, p. 107796, 2021.

[3] Z. Yan, H. Peng, X. Chen, and M. Yan, "Design, modeling, and control of electronic mechanical brake system: A review," *SAE International Journal of Vehicle Dynamics, Stability, and NVH*, vol. 8, no. 10-08-04-0026, 2024.

[4] L. Zhang, Z. Zhang, Z. Wang, J. Deng, and D. G. Dorrell, "Chassis coordinated control for full x-by-wire vehicles-a review," *Chinese Journal of Mechanical Engineering*, vol. 34, pp. 1–25, 2021.

[5] L. Yijun, T. Shim, D.-H. Shin, S. Lee, and S. Jin, "Effective clamping force control for electromechanical brake system," in *2020 IEEE/ASME International Conference on Advanced Intelligent Mechatronics (AIM)*. IEEE, 2020, pp. 643–648.

[6] J. H. Bae *et al.*, "Soft computing approach for sensorless control in brake-by-wire systems with electro-mechanical brake," Ph.D. dissertation, DGIST, 2017.

[7] C. Kim, Y. Kim, O. Kwon, J. Seo, D. Lee, and H. Yi, "An application of the brain limbic system–based control to the electromechanical brake system," *Advances in Mechanical Engineering*, vol. 10, no. 2, 2018.

[8] W. Wei, T. He, and A. Pal, "Real-time clamping force estimation of brake-by-wire system for electric autonomous vehicles," in *2023 American Control Conference (ACC)*. IEEE, 2023, pp. 1018–1023.

[9] F. Chen, H. Ouyang, and X. Wang, "A new mechanism for friction-induced vibration and noise," *Friction*, vol. 11, no. 2, pp. 302–315, 2023.

[10] G. Park and S. B. Choi, "Clamping force control based on dynamic model estimation for electromechanical brakes," *Proceedings of the Institution of Mechanical Engineers, Part D: Journal of Automobile Engineering*, vol. 232, no. 14, pp. 2000–2013, 2018.

[11] Y. Zhao, H. Lin, and F. Miao, "An adaptive backstepping nonsingular fast terminal sliding-mode control for the electromechanical brake system with backlash nonlinearity compensation," *Proceedings of the Institution of Mechanical Engineers, Part F: Journal of Rail and Rapid Transit*, vol. 237, no. 7, pp. 858–870, 2023.

[12] W. Wei, T. He, Y. Men, J. Wang, L. Xiong, and G. Yin, "Nonlinear model predictive clamping force control for electromechanical brake system," in *2024 International Conference on Advanced Robotics and Mechatronics (ICARM)*. IEEE, 2024, pp. 789–794.

[13] W. Wei, H. Dourra, and G. G. Zhu, "Adaptive transfer case clutch touchpoint estimation with a modified friction model," *IEEE/ASME Transactions on Mechatronics*, vol. 25, no. 4, pp. 2000–2008, 2020.

[14] G. Riva, D. Nava, S. Formentin, and S. M. Savaresi, "Robust force control for brake-by-wire actuators via scenario optimization," *IFAC-PapersOnLine*, vol. 53, no. 2, pp. 1–6, 2020.

[15] F. Wang, D. Chen, Y. Cai, X. Xu, and Y.-Q. Ni, "Nonlinear clamping force estimation and robust control of an electro-mechanical brake system for electric vehicles based on pwa-h," *IEEE/ASME Transactions on Mechatronics*, 2024.

[16] W. Wei, G. Yin, and T. He, "Physics-informed data-based LPV modeling and validations of lateral vehicle dynamics," *IEEE Transactions on Intelligent Vehicles*, vol. 9, no. 1, pp. 2459–2468, January 2024.